Real-time Ocean Surface Current Measurements in the Gulf of Mexico

Seth Zuckerman
Steven P. Anderson
Areté Associates
1550 Crystal Drive, Suite 703
Arlington, VA 22202
szuckerman@arete.com

Grant Stuart
Fugro GEOS
6100 Hillcroft
Houston, TX 77081

Cortis Cooper
Chevron
6001 Bollinger Canyon Road
San Ramon, CA 94583

***Abstract*—This paper reports on a series of airborne data collections we made in the Gulf of Mexico using the Remote Ocean Current Imaging System (ROCIS) to measure surface currents in real-time. ROCIS provides high spatial resolution over large areas of the ocean in a way not previously available with existing technologies. Such current measurements can be employed for improved regional ocean forecasting and a better understanding of mesoscale processes.**

I. Introduction

Accurate and timely knowledge of ocean surface currents is important for a variety of scientific and operational applications. Existing methodologies based on satellite feature tracking [1] and altimetry [2], high frequency (HF) radars [3], drifting buoys [4], and Acoustic Doppler Current Profilers [5]-[6] (ADCPs) are well established but not optimal for obtaining high spatial resolution measurements over broad areas. Satellite and HF radar techniques provide large coverage areas but have limited spatial resolution. In addition, satellite methods are limited by cloud cover and the performance of HF radars varies with environmental conditions. Drifting buoys only provide Lagrangian measurements and may drift out of the region of interest. Moored ADCPs only provide point measurements and shipboard ADCPs are limited by the speed of the vessel being used and have limited utility in high sea states.

The Remote Ocean Current Imaging System (ROCIS) was developed to provide high resolution maps of surface currents over large areas. ROCIS exploits space-time processing of airborne ocean wave imagery to produce maps of surface currents in real-time. Broad areas of the ocean can be covered during the duration of a single flight with measurements taken at a level of detail to allow small-scale circulation features to be identified.

ROCIS is an extension of previous airborne imaging systems developed to remotely sense near-shore ocean currents [7]-[8]. A previous version of the system was first flown in October 2012 over the Gulf of Mexico [9]-[10]. However, it was not real-time and required post-processing of image data to retrieve current measurements. This paper reports on our advances since then upgrading ROCIS to operate in real-time and on our multi-month deployment of the system to the Gulf of Mexico.

Section II provides an overview of the technology of the system. Section III reviews our field collections and results. Section IV discusses comparison of results to *in situ* data and the performance of ROCIS as a function of environmental parameters. Section V discusses sources of error, Section VI lessons learned, and Section VII provides a summary and conclusion.

II. Technology

A. Hardware

Low equipment and operational costs were a system design goal. ROCIS is made up of commercial-off-the-shelf (COTS) cameras and image hardware components. The system can quickly be installed into any survey aircraft with a photogrammetric hole. Fig. 1 shows the system installed on one of two King Air aircrafts used during our 2015 field collections.

ROCIS utilizes two cameras, one pointing forward and one backward, to mitigate the effect of sun glint contaminating the imagery from one direction. The cameras are 8-megapixel Prosilica panchromatic CCDs (3296 x 2472), with 18mm lenses and red filters. This yields a field of view of 54° by 40°, with the larger dimension oriented along the direction of flight to provide increased dwell.

The cameras image the water surface at 2 Hz, using a signal generated by a trigger box to synchronize both cameras with the inertial navigation system (INS). The INS is an Applanix POS-AV 410 with Fugro StarFix augmentation, which provides highly accurate real-time position and orientation information. Boresighting of the INS to the individual cameras is accomplished by flying over targets with known locations and determining offset angles through an iterative best fit process.

The data acquisition computer (DAQ) is an Intel core i7, 3.6 GHz, with 8 GB of RAM running Windows 7. Data are recorded onto 4 solid state drives (SSDs)—each camera is mirrored to its own pair of SSDs. This provides data redundancy and obviates the need to back up the data post-flight before further analysis can be started. The DAQ is controlled from a generic laptop via a remote desktop connection.

978-0-933957-43-5

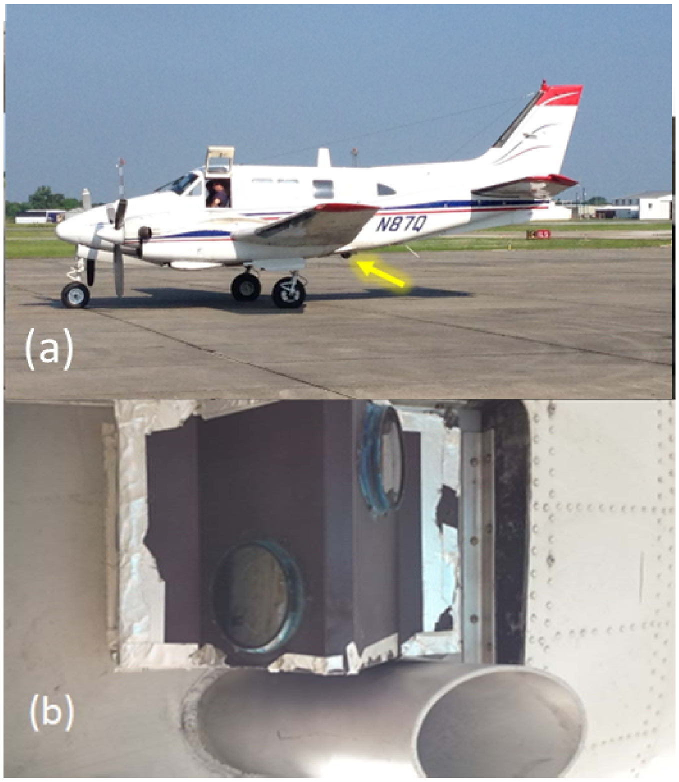

Fig. 1. (a) ROCIS installed on one of two King Air aircraft used during data collections. A yellow arrow points to the imaging payload located underneath the aircraft. (b) A view from under the aircraft showing the dual cameras pointing in opposite directions. Also visible is a tube for deploying airborne expendable bathythermographs (AXBTs) or airborne expendable current profilers (AXCPs).

B. *Software*

The real-time data acquisition and processing software is written in MATLAB using the Image Acquisition Toolbox and GigE vision protocol. Once initialized, very little operator interaction is necessary to collect images and calculate currents. The software controls the integration time for the cameras through separate auto-exposure loops. As images are received from the cameras, the software records them to the SSDs. Concurrently, synchronized position and attitude information is received from the INS over a serial port. The software then passes the images and metadata to the current retrieval algorithm (described below).

The system is configured to provide the maximum real-time spatial resolution possible while guaranteeing no lost image data. This interplay is dependent upon the underlying computer resources of the DAQ. As currently configured, the system calculates one current retrieval every 12 seconds. Given nominal flight speeds around 145 kts, this yields a retrieval every 850-1000 m along the flight path.

To minimize the processing load on the DAQ, all display and visualization of the real-time measurements is done on the control laptop. As each current retrieval is completed, it is sent to the laptop over the remote desktop connection. A graphical user interface (GUI) running on the laptop receives this information and updates the visual charts and graphs. The operator is able to view a live map of the results as well as several plots of diagnostic information to check data integrity.

C. *Current Retrieval Algorithm*

The current retrieval algorithm in ROCIS builds on prior work done using similar passive sensors [7]-[8]. The fundamental approach is to image the surface gravity waves and retrieve the currents from the observed Doppler shift. In deepwater, the motion of surface waves is described by the linear dispersion relation

$$\omega = \sqrt{gk} + \vec{k} \cdot \vec{U} \qquad (1)$$

where ω is the frequency, k is the vector wavenumber and U is the mean surface current vector. By observing the Doppler shift of the waves via the collection of frequency values for the given wavenumbers present in the scene, we can fit for the free parameter U to retrieve the current.

The first step in the retrieval process is to georeference the images to the water surface. The high accuracy of the Applanix INS is crucial for this step. Next, an image stack is built up by extracting a square patch centered at each retrieval location (typically 256 x 256 m). Adequate dwell is necessary for a good retrieval, typically between 30-120 s depending on flight speed and altitude. Once an image stack is complete, the algorithm performs a three dimensional Fourier transform and calculates the power spectral density (3D-PSD).

The wave energy in the 3D-PSD lies along the two dimensional surface described by (1). A nonlinear least squares fit is performed to derive the current vector U. In addition, a goodness of fit value is estimated, which can later be used as an error metric to filter out wild points.

III. Data Collections

We flew ROCIS in the Gulf of Mexico from February to June 2015 for a total of 137 flights. Typical flights covered around 1000 km in 4 hours at altitudes ranging from 900 m to 2100 m. Fig. 2 shows the real-time current measurements from March 29, 2015. The coastline of southern Louisiana is shown at the top of the map. The cyclonic flow of the Loop Current in this region is visible in detail. We flew near daily and sometimes twice daily flights, providing a unique and unprecedented view of the Loop Current in this region and its evolution during this time span. Throughout the course of our data collections we observed the Loop Current migrate several hundreds of kilometers, as well as saw a large eddy break free and later reattach to the main flow.

Flight altitude is dependent on the cloud cover in the region of operation. The optimal altitude for flying ROCIS is 2100 m. At flight speeds of around 145 kts, this provides 120 s of dwell for each patch. However, during many of our data collections cloud cover below 2100 m forced the aircraft to fly lower (as low as 900 m) to operate below the cloud deck, decreasing the dwell. Longer dwells yield more accurate current retrievals since the frequency of the waves is better sampled. A more detailed discussion of the effect of clouds on the current retrievals is presented in Section V.

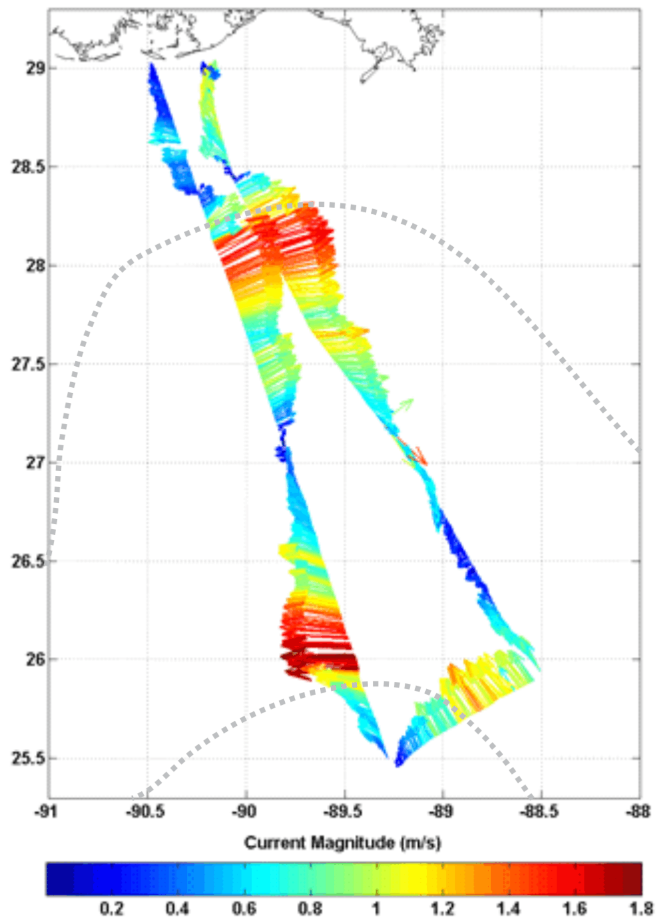

Fig. 2. ROCIS real-time current measurements from March 29, 2015. The detailed structure of the Loop Current is visible, with currents reaching 1.8 m/s at maximum. Dashed lines indicate the location of surface temperture fronts.

In an operational setting, the real-time current measurements are the most important data product ROCIS provides. However, since all of the image data are recorded to disk, several more advanced analyses can be undertaken using post-processing software. Currents can be retrieved at higher spatial resolutions than in real-time, either in a single line or grid. During the course of system development and testing we used such analyses to carry out sensitivity studies to determine the optimal algorithm parameters for use in real-time collections.

Additionally, the swaths of currents that post-processing provides are useful for the investigation of mesoscale ocean features. Fig. 3 shows one example of swath current retrievals at Southwest Pass, where the detailed structure of the Mississippi outflow is visible. ROCIS can provide vectors over a swath up to 4 km across the flight track with spatial resolution of 250 m or less depending on flight altitude. Such swath data is valuable for the analysis of coherent features, statistical and Fourier analysis, estimation of convergence and vorticity, and assimilation into numerical models.

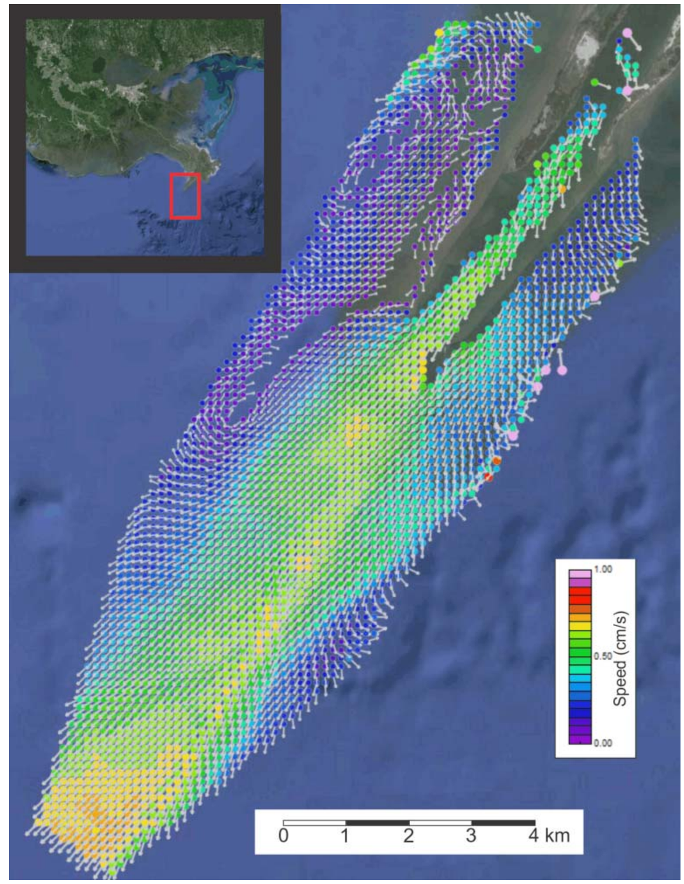

Fig. 3. ROCIS post-processed currents over the Mississippi River outflow at Southwest Pass. Currents were calculated on a grid of 128 x 128 m non-overlapping tiles. Current retrievals span a swath of 4 km across-track.

IV. System Performance

On several occasions during the course of our field collections ROCIS flew close to an ocean and atmospheric monitoring buoy located at N26.6698°, W90.4698°. This provided an opportunity for an *in situ* comparison and environmental characterization.

The current monitoring instrument on this buoy is an Aanderaa Doppler Current Sensor (DCS). It provides a point measurement at a depth of 1.5 m. ROCIS flew within 5 km of the DCS on 53 separate flights. For each flight, the closest real-time current measurement to the buoy was chosen as a comparison point. The scatter plot comparison is shown in Fig. 4. We found excellent agreement between the DCS and ROCIS real-time data. RMS errors were 0.16 m/s in magnitude and 15.9° in direction. The bias values were 0.08 m/s in magnitude and -2.5° in direction.

Data from the buoy also provided knowledge of the environmental conditions present while ROCIS was operating. Using the same 53 time periods as above, wind speeds ranged from 1 m/s to 14 m/s and significant wave heights ranged from 0.16 m to 3.2 m. Thus, ROCIS was able to successfully retrieve ocean currents in a wide range of wind and sea conditions.

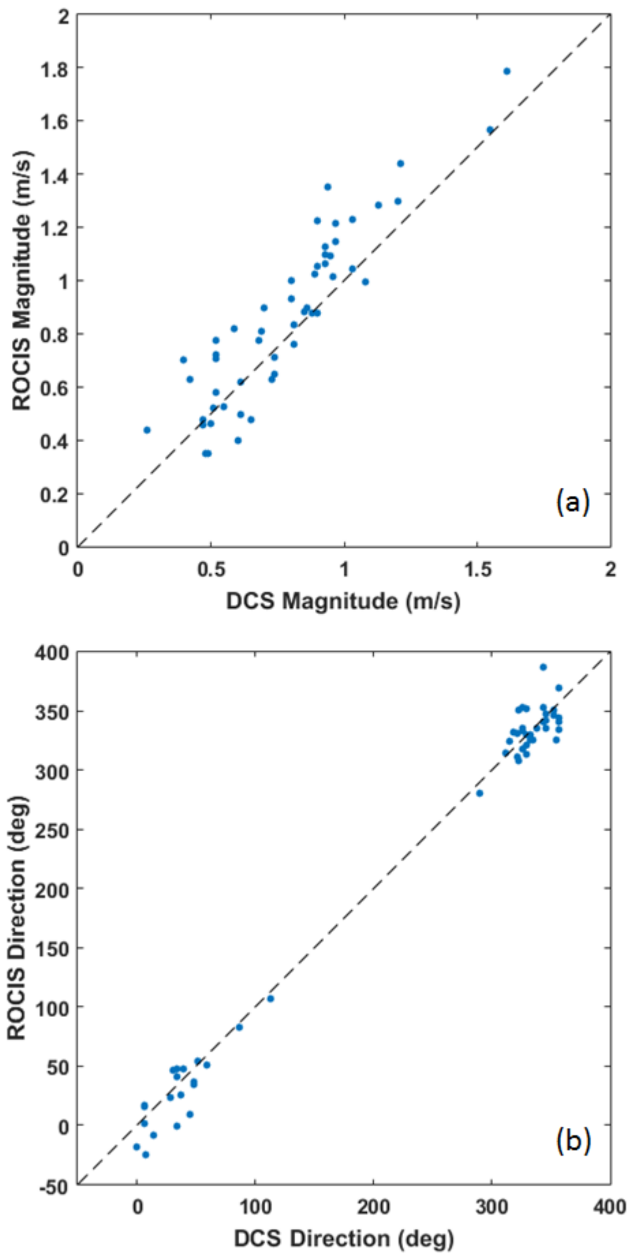

Fig. 4. *In situ* comparison: ROCIS real-time currents vs. DCS current measurements. ROCIS flew within 5 km of the DCS 53 times during our data collections. Panel (a) shows the magnitude comparison, with a RMS error of 0.16 m/s and bias of 0.08 m/s. Panel (b) shows the direction comparison, with a RMS error of 15.9° and a bias of -2.5°.

V. Sources of Error

A. Clouds

Scattered clouds below the aircraft up to 50% still allow for excellent retrievals. Since the plane is moving quickly relative to the clouds, each individual cloud only fills up a few frames of data, saturating the majority of the pixels. In between these saturated frames, the rest of the frames in the image stack are still of high quality. The 3D-PSD is computed as normal, and energy due to the presence of clouds lies along a vertical stack at the origin, spanning all frequencies near zero wavenumber.

The current fitting algorithm only looks for wave energy described by the model in (1) and effectively ignores any additional energy in the 3D-PSD due to the clouds. However, beyond approximately 50% cloud cover there are not enough good images of the ocean waves and the SNR of wave energy along the dispersion surface rapidly deteriorates. Since the model in (1) no longer fits the observed data in the 3D-PSD this leads to wild points—retrievals with high goodness of fit values that are easily discarded.

Thus, clouds are not a significant limitation for successful current measurements with ROCIS. For all missions, the aircraft approached the survey region expecting to fly at the optimal altitude of 2100 m. Upon reaching the survey region, the operator and pilots assessed the cloud cover in the area and determined if a change of altitude was necessary.

B. Nonlinear Fit

A small amount of error is introduced into the current measurement due to the necessity of performing a nonlinear least squared fit. When a broad band of waves are present, as is almost always the case in the open ocean, it is common to have 1000-2000 data points in the nonlinear fit, yielding a small error due to the fit process itself on the order of 1-2 cm/s.

The fit error increases for two reasons: short dwell and low wave SNR. Shorter dwell, between 30-40 s, causes the frequency resolution of the 3D-PSD to greatly decrease. The frequency of the waves used in the fit is known less precisely, and the resulting fit error of the velocity increases slightly. By artificially shortening the dwell of an image stack with full dwell, we have shown this additional increase in fit error to be on the order of 3-5 cm/s.

If the wave SNR is prohibitively low (usually below 12 dB) due to the presence of excess cloud cover, sun glint, white caps, or a sufficiently narrow banded wave field, the fit error will increase greatly. As above, this is due to the observed data in the 3D-PSD not fitting the model described by (1). In such cases, the fit error can be quite large, though such wild points are easily flagged and discarded.

C. Georeferencing

Georeferencing errors include errors in the absolute measurement of the camera's attitude and position, errors in the boresight offsets between the cameras and inertial measurement unit (IMU), and error due to using an incorrect water surface height. Georeferencing errors cause frame-to-frame drift in the image stack and bias the resulting current measurement in the direction of the drift.

Errors in the absolute estimation of the camera's attitude and position are always present. However, using a high-performance INS system such as the Applanix POS-AV 410 minimizes these errors. In addition, we operated with Fugro StarFix augmentation for further GPS accuracy over the ocean. As such, we found these errors to have a negligible effect on the resulting current measurements.

After installing the system, a calibration flight over the airport is flown to image targets (runway lights), whose locations have previously been measured with survey GPS equipment. Using this data, the offset angles between the cameras and IMU are estimated through an iterative best fit process. In our experience, these offset angles must be known to an accuracy of ±0.05° or drift will appear in the image stacks. We verified the accuracy of the calculated offsets by creating movies of georeferenced images either over the airport itself or over the beach the aircraft passed over on its way out to the survey region. In both instances, the surface height of the land was known from prior GPS measurements. In this way, any drift in the movie is solely due to errors in the offset angles. If excessive drift is present, then a recalculation of the offset angles is needed. Thus, through this iterative process errors due to inexact knowledge of the offset angles are reduced and made negligible.

Currently, imprecise knowledge of the water surface height is a large contributing factor to retrieved current error. The water surface height used in the algorithm is extracted from the geopotential Earth Gravitational Model 1996 (EGM96). This is a static ocean surface model, but the open ocean topography is modulated by tides and mesoscale variability which are not accounted for at this time.

A surface height error causes a drift in the image stack in the along-track direction, either toward or away from the direction of flight depending on whether the surface height is over- or under-valued. This drift vector is an additive error to the underlying current vector, and is inversely proportional to flight altitude. Theoretical calculations suggest that a 1 m height error produces a 1.7 cm/s along-track current error at 2100 m but a 4.0 cm/s error at 900 m. Qualitatively, we have observed higher point-to-point noise in the retrieved currents from flights at lower altitudes than higher altitudes. Ongoing efforts are underway to better quantify this result.

VI. Lessons Learned

A. Real-time Measurements

Though more complicated analyses will always require post-processing of image data, we found several important benefits to having real-time processing and visualization. First, data quality checks can happen in real-time instead of waiting until after landing. The operator is able to visualize the current vectors as they are calculated. If several vectors in a row are erroneous, this may be an indication that an algorithm parameter needs adjustment. Additionally, the operator can redirect the aircraft in stride to focus on particular ocean features of interest. Lastly, and most importantly, real-time processing provides rapid data distribution to end-users. Immediately upon landing, a text file with measurements can be uploaded to a data server for timely regional ocean forecasting.

B. Aircraft Operations

Five months of near daily flights required intensive manpower from both operators and pilots. Crews were regularly switched out after 2-4 weeks in the field. In addition, FAA aircraft regulations required maintenance to be performed after 100 hours of flight which occurred approximately once a month. To accommodate this requirement while not losing 7-10 days of collections, two aircraft were used and the imaging payload was moved back and forth. Each move required a recalibration of the cameras as we found that the boresight offset angles changed by more than 0.05° with each reinstallation.

ROCIS from an unmanned aerial vehicle (UAV) is a long-term option. UAV flight speeds are much slower than the King Air, which will allow for much lower flight altitudes to achieve similar dwells. The UAV could be launched directly from a boat or other offshore platform. Since the UAV would already be in the survey region, data coverage would be approximately equal to that of a manned aircraft, which requires extensive transit distances.

UAVs can be used for near-shore wave imaging where land in the scene is used for image registration [11]. For offshore applications, the limiting technology is the class of INS available on such UAVs, which are not accurate enough for direct current measurements. However, we believe that within five years the technology will exist to operate ROCIS from a UAV.

VII. Conclusions

ROCIS exploits space-time processing of ocean wave imagery to produce maps of surface currents in real-time. Real-time currents have high spatial resolution over large areas and are collected in a matter of hours. Post-processing of the imagery data creates additional data sets with swaths of currents useful for investigating a variety of mesoscale features. The system is made from COTS components and is designed to be quickly installed on any survey aircraft.

From February to June 2015, we flew near daily flights over the Loop Current in the Gulf of Mexico. On several occasions we flew over an *in situ* buoy. A current comparison with a DCS yielded good agreement, and environmental data showed the range of wind and wave conditions that ROCIS is able to successfully operate under.

ROCIS is well suited to operational missions such as search and rescue and oil spill response, where timely knowledge of surface currents is crucial. As UAV technology improves, ROCIS technology will migrate to small fixed wing UAVs for cheaper and safer data collections.

Acknowledgment

At Areté Associates, we thank all our colleagues who have helped with various parts of system development, testing, and field collections. At Fugro GEOS, we thank all of the very capable system operators who admirably handled several months of continuous data collections. We thank all of the pilots at Dynamic Aviation who expertly flew daily, and often twice-daily, missions. For *in situ* buoy data, we thank Petrobras America, Inc. Lastly, we especially thank John Dugan for his friendship and pioneering research on optical imaging of the marine environment.

References

[1] W. J. Emery, A. C. Thomas, M. J. Collins, W. R. Crawford and D. L. Mackas, "An objective method for computing advective surface velocities from sequential infrared satellite images," *J. Geophysical Research*, vol. 91, pp 12 865-12 878, November 1986.

[2] R. Leben, G. Born and B. Engegreth, "Operational altimeter data processing for mesoscale monitoring," *Marine Geodesy*, vol. 25, pp. 3-18, February 2002.

[3] J. D. Paduan and L. K. Rosenfeld, “Remotely sensed surface currents in Monterey Bay from shore-based HF radar (Coastal Ocean Dynamics Application Radar),” *J. Geophysical Research Atmosphere*, vol. 101, pp. 20 669-20 686, September 1996.

[4] S. P. Anderson and N. Sharma, “Satellite-tracked drifter measurements of inertial currents in the Gulf of Mexico,” *Current Measurement Technology*, Charleston, SC, 2008, pp. 285-288.

[5] S. P. Anderson, C. K. Cooper, D. B. Driver and J. van Smirren, “EddyNet: a measurement program for collecting real-time current profiles from the Gulf of Mexico,” *Current Measurement Technology*, San Diego, CA, 2003, pp. 277-281.

[6] S. P. Anderson and P. Matthews, “A towed 75 KHz ADCP for operational deepwater current surveys,” *Current Measurement Technology*, Southampton, UK, 2005, pp. 46-49.

[7] J. P. Dugan and C. C. Piotrowski, “Surface current measurements using airborne visible image time series,” *Remote Sens. Environ.*, vol. 84, pp. 309-319, February 2003.

[8] J. P. Dugan and C. C. Piotrowski, “Accuracy of bathymetry and current retrievals from airborne optical time series imaging of shoaling waves,” *IEEE Trans. Geosci. Remote Sens.*, vol. 40, pp. 2606-2618, December 2002.

[9] S. P. Anderson, S. Zuckerman, S. Fan, and J. van Smirren, “Airborne optical remote sensing of ocean currents,” *Oceans*, San Diego, CA, 2013, pp. 1-7.

[10] S. Zuckerman and S. P. Anderson, “Advances in passive remote sensing of ocean currents and depths,” *IEEE Int. Geoscience and Remote Sensing Symp.*, Quebec City, Quebec, Canada, 2014, pp. 3906-3909.

[11] R. A. Holman, K. T. Holland, D. M. Lalejini, and S. D. Spansel, “Surf zone characterization from unmanned aerial vehicle imagery,” *Ocean Dynamics*, vol. 61, pp. 1927-1935, June 2011.